doi:10.1246/cl.2011.668
Published on the web June 4, 2011

Highlight Review

Aqueous Lithium/Air Rechargeable Batteries

Tao Zhang, Nobuyuki Imanishi,* Yasuo Takeda, and Osamu Yamamoto

(Received March 1, 2011; CL-118006)

Abstract

Several key issues of aqueous lithium/air rechargeable batteries that consists of a water-stable lithium electrode, an aqueous electrolyte, and a bifunctional air electrode are reviewed. Based on research and discussion of these issues, the challenges and prospects for high energy density aqueous lithium/air rechargeable batteries are described. From a broader perspective, lithium/air rechargeable batteries that employ aprotic electrolytes are also briefly introduced for comparison.

♦ Introduction

During the past few years, lithium/air rechargeable batteries have received significant attention, due to their potential for development as a high energy density battery for electric vehicles (EVs). The number of research papers on lithium/air batteries has increased year by year. The sharp increase in interest is motivated by the high theoretical energy density of lithium/air batteries (11140 $W\,h\,kg^{-1}$, excluding oxygen), which is comparable with that of 13000 $W\,h\,kg^{-1}$ for gasoline[1] and such an energy density would be applicable for EV batteries with an acceptable driving range. There is high expectation for high energy density lithium/air batteries to serve as power sources to drive pure EVs, which would contribute to a reduction in global greenhouse gas emissions and address the crisis of fossil energy source exhaustion.

Two types of lithium/air batteries have been studied, nonaqueous and aqueous electrolyte systems. Two possible cell reactions for the nonaqueous electrolyte system are

$$2Li + O_2 \rightleftarrows Li_2O_2 \quad (1)$$

$$\text{and} \quad 2Li + 1/2O_2 \rightleftarrows Li_2O \quad (2)$$

The reversible cell voltages for reactions (1) and (2) are 2.959 and 2.913 V, respectively. It has been demonstrated that reaction (1) is reversible, whereas reaction (2) is irreversible.[2] The energy density of 3456 $W\,h\,kg^{-1}$ (including oxygen) is calculated using reaction (1). In an aqueous electrolyte, water molecules are involved in the reaction according to the following reaction:

$$4Li + 6H_2O + O_2 \rightleftarrows 4(LiOH\cdot H_2O) \quad (3)$$

The reversible cell voltage for reaction (3) is 3.84 V in a neutral solution, and the energy density (including oxygen) is 2450 $W\,h\,kg^{-1}$. The energy density of the aqueous system is approximately 30% lower than that of the nonaqueous system (including oxygen).

It is well known that lithium reacts vigorously with water to produce LiOH and hydrogen gas. Therefore, to avoid this parasitic reaction, most research on lithium/air batteries have focused on using aprotic organic solvents as electrolytes. In the case of using aprotic electrolytes, Bruce and colleagues have given a preliminary demonstration using gravimetric analysis and in situ mass spectrometry that Li_2O_2 formed upon discharge was decomposed to Li and O_2 during a charge cycle, both with and without a catalyst.[2] However, there are some severe problems that must still be addressed, such as lithium corrosion by water and CO_2 ingression when operated in air (poor lifetime), precipitation of Li oxides on the porous cathode (low capacity), and high polarization resistance of the air electrode (low energy conversion efficiency). These problems could be removed by using a water-stable lithium electrode (WSLE) and an aqueous electrolyte.

Recently, two reviews on lithium/air batteries[3] were published that focused on nonaqueous lithium/air batteries; however, only a few results were given with respect to the aqueous electrolyte system. In this review, several key issues for the development of aqueous lithium/air rechargeable batteries will be emphasized. Part one of this review will introduce the WSLE, which is a key part of the aqueous lithium/air system and is also useful for the nonaqueous system to protect from the contamination of lithium from water in air. In part two the reversibility of the cell reaction with aqueous electrolytes and the bifunctional catalysts for the oxygen reduction and the oxygen evolution is discussed, and part three compares the aqueous and nonaqueous lithium/air systems. The conclusion section summarizes the challenges to realize a practical aqueous lithium/air secondary battery.

♦ Water-stable Lithium Electrodes

The prerequisite to obtain a practical aqueous lithium/air secondary battery is the development of a WSLE that can survive lithium stripping/deposition for a long lifespan in an aqueous electrolyte. This type of electrode was preliminarily addressed by the concept of a composite lithium anode with a three-layer construction proposed by Visco et al. in 2004.[4] This electrode concept adopts a water-stable NASICON (Na^+ superionic conductor)-type lithium-conducting solid glass ceramic as a protective layer that covers and isolates the lithium metal from direct contact with the aqueous electrolyte. At present, most research on WSLEs has utilized the $Li_{1+x+y}Ti_{2-x}Al_xP_{3-y}Si_yO_{12}$ (LTAP) glass ceramic provided by Ohara Inc., Japan.[5] A typical LTAP plate has a thickness of ca. 260 μm and an ionic conductivity of 3.5×10^{-4} $S\,cm^{-1}$ at 25 °C and

Dr. Tao Zhang, Prof. Nobuyuki Imanishi, Prof. Yasuo Takeda, and Prof. Osamu Yamamoto*
Department of Chemistry, Faculty of Engineering, Mie University, 1577 Kurimamachiya-cho, Tsu, Mie 514-8507
E-mail: imanishi@chem.mie-u.ac.jp

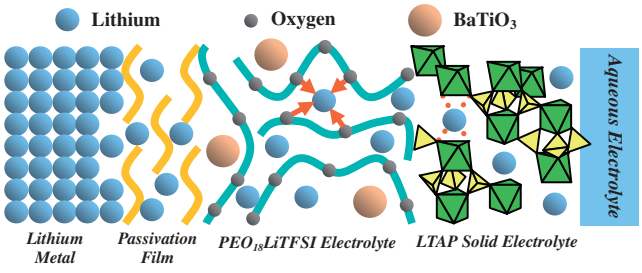

Figure 1. Schematic diagram of the proposed WSLE with $PEO_{18}LiTFSI–BaTiO_3$ buffer layer and LTAP (from Zhang et al., ref 9).

$1.4 \times 10^{-3}\,S\,cm^{-1}$ at 60 °C.[6] However, LTAP is unstable in direct contact with lithium metal, so that a buffer layer must be used between the lithium metal and LTAP plate.

Selection of Buffer Layer.

The buffer layer should have high lithium ion conductivity and be stable in contact with lithium metal. Visco et al. proposed the deposition or evaporation of lithium-conducting solid materials such as Li_3N or $Li_3(P,N)O_3$ onto the LTAP plate by a variety of techniques, including RF sputtering, e-beam evaporation, and thermal evaporation.[7] The electrical conductivity of Li_3N at room temperature is as high as $10^{-3}\,S\,cm^{-1}$;[8] however, these methods for preparation of a protective layer are complicated and too expensive for scale-up.

Lithium-conducting polymer electrolytes are the other promising candidate for the buffer layer. We have previously proposed a buffer layer based on an electrolyte consisting of poly(ethylene oxide) (PEO) with the $Li(CF_3SO_2)N$ (LiTFSI) (O/Li = 18/1) lithium salt, due to its chemical compatibility with Li and LTAP.[9] A typical WSLE construction with a PEO-based electrolyte as the buffer layer is shown in Figure 1. The ionic conductivity of $PEO_{18}LiTFSI$ is $5 \times 10^{-4}\,S\,cm^{-1}$ at 60 °C.[9] The bulk conductivity of PEO can be increased by the addition of nanosized ceramic fillers such as Al_2O_3, SiO_2, and $BaTiO_3$[9,10] or room-temperature ionic liquids such as *N*-methyl-*N*-propyl-piperidinium TFSI (PP13TFSI).[11] In addition to the high conductivity and good compatibility with lithium metal, the interfacial resistance between lithium and the polymer electrolyte and between the polymer electrolyte and LTAP is also of significant importance. In addition, dendrite formation during lithium deposition during charging is an inevitable problem.[12]

Interfacial Resistance and Dendrite Formation.

The interfacial resistance of the WSLE is somewhat complicated. Typical impedance spectra of $Li/PEO_{18}LiTFSI–10\,wt\%BaTiO_3/LTAP$/aqueous LiCl solution/Pt are shown in Figure 2. A small semicircle is apparent at high frequency and a large semicircle at low frequency. Analysis of the impedance profiles indicates that the small semicircle corresponds to the polymer electrolyte and LTAP grain boundary resistances and that the large semicircle represents the resistance of a passivation film, the interfacial resistance between the polymer electrolyte and LTAP, and the charge-transfer resistance.[9] Comparison of the impedance of $Li/PEO_{18}LiTFSI/LTAP$ and $Li/PEO_{18}LiTFSI$

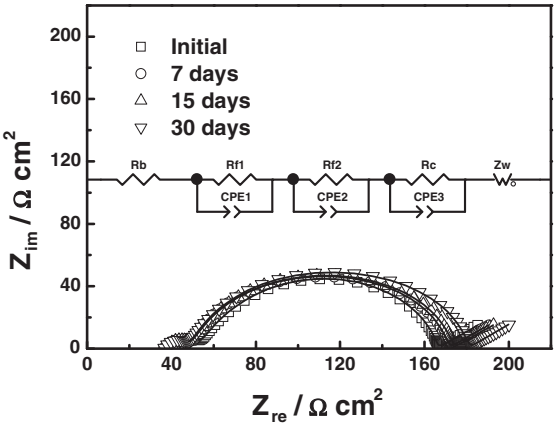

Figure 2. Time dependence of the impedance spectra of $Li/PEO_{18}LiTFSI–10\,wt\%BaTiO_3/LTAP/1$ M aqueous LiCl/Pt, air at 60 °C.

Table 1. Li/polymer interfacial resistance (at 60 °C) in a Li/polymer/Li symmetric cell relative to the average size and BET surface area of the corresponding nanofiller

	$PEO_{18}LiTFSI$	$BaTiO_3$		Al_2O_3	SiO_2	PP13TFSI
Size/nm	—	100	40	35	50	—
BET/$m^2\,g^{-1}$	—	5.50	6.68	27.25	67.66	—
$R_i/\Omega\,cm^2$	240	125	38	80	54	49

symmetric cells (Figure S1[40]) indicates that the interfacial resistance calculated for $PEO_{18}LiTFSI/LTAP$ is ca. 40% that of the $Li/PEO_{18}LiTFSI$ interface. The high interface resistance between lithium and a polymer electrolyte has been known to be reduced by addition of oxide fillers.[9,10] The addition of PP13TFSI to $PEO_{18}LiTFSI$ has also been shown to decrease the interfacial resistance.[11] Table 1 provides examples of the interface resistance between lithium and $PEO_{18}LiTFSI$ with various oxide fillers or PP13TFSI. These results indicate that the addition of a $BaTiO_3$ (40 nm) nanofiller significantly reduces the interfacial resistance of $Li/PEO_{18}LiTFSI$ from 240 to 38 $\Omega\,cm^2$. Several reports[10] have suggested that the addition of nanofillers significantly reduces the growth rate of the lithium passivation layer, probably due to the trapping of residual impurities that promote the formation of compact thin passivation layers on the Li/polymer interface.

Lithium dendrite formation has been observed for the WSLE during repeated discharge/charge. In the early stage of lithium battery research, lithium metal was mostly used as an anode material. There have been many reports regarding the severe lithium dendrite formation experienced with conventional organic electrolytes;[12,13] therefore, such organic electrolytes may be not suitable for the protective layer between lithium and LTAP. Lithium dendrite formation can be suppressed by using a polymer electrolyte. The mechanism of dendrite growth in Li/polymer electrolyte/Li has been extensively studied by Brissot et al.[14] with the aid of a direct in situ observation technique and simultaneous cell potential evaluation. We have also recently employed a visualization cell and found that acid-modified nano-SiO_2[15] and PP13TFSI[11] additives to the $PEO_{18}LiTFSI$ buffer layer exhibit excellent effects for the suppression of lithium dendrite formation. Table 2 shows the results for dendrite

Table 2. Dendrite formation onset time and the capacity of lithium electrode with a 10-μm thick copper current collector (from Liu et al., ref 11)

Electrolyte	Temp. /°C	Current density /mA cm^{-2}	Onset time /h	Capacity /mA h g^{-1}
$PEO_{18}LiTFSI$	60	0.5	15	688
		0.1	125	1025
$PEO_{18}LiTFSI$–1.44PP13TFSI	60	1.0	17	1270
		0.5	35	1300
EC–DMC–EMC–$LiPF_6$	15	1.0	0.2	22
PAN–PC–EC–$LiPF_6$	Room temp	1.0	1	100

formation at the interface of lithium and various electrolytes. The capacity of the cell using a liquid electrolyte, which was counted by the weight of a 10-μm thick copper current collector and the weight of lithium deposited up to the onset time of dendrite formation, was much lower than that of the cell using a polymer electrolyte. The onset time of lithium dendrite formation was increased from 15 to 35 h at 0.5 mA cm^{-2} by the addition of PP13TFSI into $PEO_{18}LiTFSI$ up to 1.44 mol, which corresponds to a specific capacity of 1300 mA h g^{-1}. This capacity is acceptable for an anode in lithium/air batteries.

Stability of WSLE in Aqueous Electrolytes.

The stability of WSLE in aqueous electrolytes is dependent on the sealing technology and the tolerance of LTAP to the aqueous electrolyte. The stability of the LTAP plate in aqueous acidic/alkaline electrolytes has been studied in detail.[16] Figure 3 shows scanning electron microscopy (SEM) images of LTAP plate that was immersed in aqueous solutions of various pH at 50 °C for 3 weeks. Conductivity measurements revealed that LTAP plate was unstable in aqueous acid and alkaline solution but was more stable in lithium ion-saturated solutions, such as $LiCH_3COO$ saturated CH_3COOH–H_2O solution[17] and LiCl-saturated LiOH solution.[16] Table 3 summarizes the electrical conductivity of LTAP plates immersed in various LiCl–LiOH–H_2O solutions at 50 °C for 3 weeks. The stability of LTAP in the LiCl-saturated aqueous LiOH solution suggests the possibility to develop an aqueous lithium/air battery with high energy density, because the reaction product is LiOH and the electrolyte is saturated with LiOH at deep discharge.

Weppner and colleagues reported a new garnet-type lithium ion-conducting solid electrolyte of $Li_7La_3Zr_2O_{12}$ that exhibited a high ionic conductivity of 2.4×10^{-4} S cm^{-1} at 25 °C and stability with lithium.[18] We recently reported[19] that $Li_{7-x}La_3Zr_2O_{12-1/2x}$ is stable in the LiCl-saturated aqueous solution. The stability of this promising solid electrolyte with lithium metal should be further investigated, because a high polarization for $Li/Li_7La_3Zr_2O_{12}/Li$ was observed at a limited current density.[20]

♦ Reversibility of Aqueous Lithium/Air Battery

The high potential of lithium/air batteries at 3.8 V means

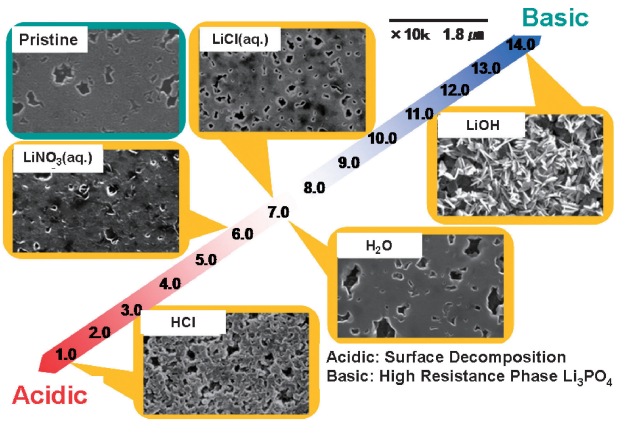

Figure 3. SEM images of LTAP immersed in various aqueous solutions at 50 °C for 3 weeks.

Table 3. Electrical conductivity of the LTAP plate immersed in various LiCl–LiOH–H_2O solutions at 50 °C for 3 weeks (from Shimonishi et al., ref 16c)

LiOH/mol L^{-1}	LiCl/mol L^{-1}	pH	Conductivity at 25 °C /S cm^{-1}
0.57	0	—	0.27×10^{-4}
0.057	0	12.78	0.58×10^{-4}
0.0057	0	11.91	1.7×10^{4}
0.00057	0	10.91	2.0×10^{-4}
3.6	8.1	9.53	2.51×10^{-4}
5.0	11.8	8.25	2.61×10^{-4}
2.3	10.4	7.64	2.55×10^{-4}

that there is some concern regarding the stability of aqueous lithium/air batteries. It may simply be regarded that water will decompose at such a high cell voltage. However, the Li/$PEO_{18}LiTFSI$/LTAP/1 M aqueous LiCl solution/Pt cell showed a stable cell voltage of 3.80 V for a long period over 3 months and good charge–discharge performance.[9]

Electrochemical Window of Aqueous Electrolytes.

The electrochemical window of aqueous electrolytes can be analyzed by the Pourbaix diagram shown in Figure 4a. Water is usually regarded to be stable in area A, which is well known as the electrochemical window of water, based on the following two electrode reactions:

$$2H^+ + 2e^- \rightleftarrows H_2 \quad E_0 = 0.00\,V \tag{4}$$

$$1/2O_2 + 2H^+ + 2e^- \rightleftarrows H_2O \quad E_0 = 1.229\,V \tag{5}$$

If a stable electrode such as Pt, Au, or carbon is inserted into the aqueous electrolyte, the theoretical electrochemical window can be easily identified by area A. However, if an active electrode such as lithium metal is placed into the aqueous electrolyte, the following reaction occurs:

$$2Li^+ + 2e^- \rightleftarrows 2Li \quad E_0 = -3.040\,V \tag{6}$$

The cell potential with a neutral solution is 3.856 V vs. the oxygen electrode, and water decomposes spontaneously. On the

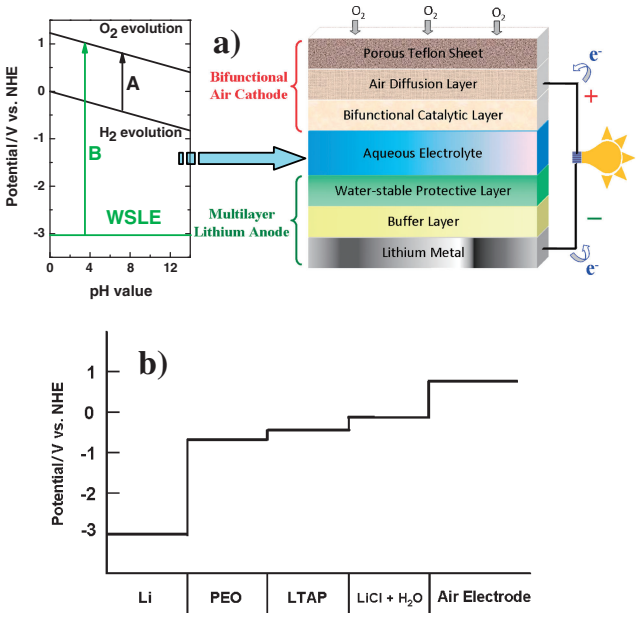

Figure 4. a) Pourbaix diagram, schematic of the aqueous lithium/air secondary batteries and b) the potential change in WSLE with aqueous electrolyte.

other hand, in the case of the WSLE, lithium metal contacts the lithium-conducting polymer electrolyte; therefore, the potential between lithium metal and the polymer electrolyte is 3.040 V. The decomposition potential of $PEO_{18}LiTFSI$ is higher than 3.8 V,[21] so that the polymer electrolyte is stable in contact with lithium metal. The interface between the polymer electrolyte and LTAP and between LTAP and the aqueous electrolyte may exhibit some junction potentials, because the lithium ion transport numbers of these electrolytes are different; however, these junction potentials are not so high. Therefore, the potential between the aqueous electrolyte and air electrode is less than 1.22 V. The change in the cell potential of $Li/PEO_{18}LiTFSI/LTAP$/aqueous LiCl solution/Pt is also shown in Figure 4b. A stable cell potential of approximately 3.8 V was observed for a long period, which corresponds to the much wider electrochemical window of area B in Figure 4a.

Meanwhile, Zhou and colleagues proposed a concept of hybrid electrolytes, which essentially employed the same LTAP plate to separate the aqueous electrolyte for cathode and the nonaqueous electrolyte for Li anode.[22] A preliminary lithium–air fuel cell using 1 M $LiClO_4$ in EC&DMC/LTAP/O_2 saturated 1 M aqueous $LiNO_3$ solution has demonstrated that the cycle between Cu and Cu_2O can be used to catalyze O_2 electrochemical reduction.[23] However, in the efforts to develop a rechargeable battery system using the hybrid electrolytes,[24] the lithium dendrite formation related to the organic electrolyte needs to be paid more attention.

Bifunctional Electrodes.

Bifunctional oxygen/air electrodes are considered for the development of rechargeable lithium/air batteries. The study of rechargeable metal/air batteries with alkaline solutions started in the middle of the 1960s. Bifunctional oxygen electrodes consume oxygen during discharge, while oxygen is evolved during charging. The bifunctional oxygen electrode developed by Simens Corp. in the early 1970s for rechargeable zinc/air batteries is composed of two layers: one of which is a hydrophobic porous nickel sheet adjacent to the electrolyte, and the other one bordering the gas phase consists of a hydrophobic carbon layer.[25] During the oxygen reduction reaction (ORR) the carbon layer plays an active role, while the nickel layer catalyzes the electrode process in the oxygen evolution reaction (OER). The activity of the carbon electrode was increased by addition of silver ($>0.96\,mg\,cm^{-2}$). These electrodes have a life of slightly more than 100 cycles.[25] The electrochemical reaction kinetics of oxygen is rather low in both aqueous acidic and alkaline electrolytes. Recently, Burchardt[26] developed a bifunctional electrode based on a hydrophobic gas diffusion layer composed of 65% porous carbon + 35% poly(tetrafluoroethylene) (PTFE), an active layer composed of hydrophobic and hydrophilic pores containing 10–30% catalyst ($MnSO_4 + La_2O_3$ or $MnO_2 + La_2O_3$) + 50–60% carbon black + 15% PTFE. This configuration is beneficial to optimize the ORR and OER catalysts with respect to their distinct requirements in the catalytic mechanism and with respect to overpotential tolerance. However, the complexity of the system is still problematic. In particular, during a long period of discharge/charge, if the aqueous electrolyte infiltrates into the ORR layer or penetrates excessively into the ORR + OER layer, both the discharge and charge capacities will quickly fade. For application to EVs, an effective design of the battery system should discharge during acceleration or cruise and be charged by regenerative braking. Therefore, all components of the bifunctional cathode must tolerate the recurrent and rapid changes of potential and current density. Therefore, it should be more beneficial for the uniformity and stability of a battery system to simplify the design, that is, use a single electrode with a single catalytic layer for simultaneous ORR and OER. Such an effective bifunctional catalyst electrode would have at least two primary features: to maintain catalytic activation for both the ORR and OER within a relatively wide overpotential range and an appropriate hydrophobic and hydrophilic balance to satisfy the oxygen diffusion/evolution over a long period. This bifunctional catalyst configuration represents an ideal direction that should significantly influence the development of EVs.

Research on bifunctional catalysts has, until now, been focused mainly on perovskite, spinel, and pyrochlore catalysts. Figure 5 shows polarization curves of bifunctional air cathodes in 7 M aqueous KOH solution.[27] The current densities for the ORR were as large as approximately $200\,mA\,cm^{-2}$ at −150 mV for all bifunctional catalysts except for that of $B' = Cu$, which had an exceptionally small surface area. Compared with the ORR, the OER activity was more dependent on the B′ cations, resulting in the following order of activity at +600 mV: Fe > Co > Ni > Mn. The OER current density with $B' = Fe$ reached $300\,mA\,cm^{-2}$ at 620 mV. Unfortunately, the Co-based catalysts were found to be unstable in alkaline solutions.[28] Thus, the Co-free perovskites of $La_{1-x}A'_xFe_{1-y}Mn_yO_3$ (A′ = La, Ca, Sr, and Ba), which exhibited both chemical stability and bifunctional activity, were studied further. The OER activity was strongly dependent on the A′ cations, resulting in the order of Sr > Ca ≫ Ba ≫ La. The HO_2^- decomposition reaction was

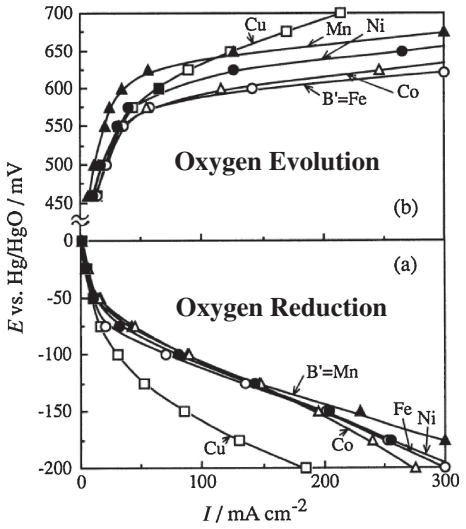

Figure 5. Polarization curves of bifunctional air cathodes using PTFE-bonded carbon loaded with 25% $La_{0.6}Ca_{0.4}Co_{0.8}B'_{0.2}O_3$ (B′ = Mn, Fe, Co, Ni, and Cu) in 7 M KOH at 25 °C. Pt-plate counter electrode and Hg/HgO (KOH) reference electrode (from Shimizu et al., ref 29).

found to be the rate-determining step for $La_{1-x}Ca_xFe_{0.8}Mn_{0.2}O_3$ in both the ORR and OER processes.[29]

Ruthenium-based pyrochlores are also quite effective catalysts for the ORR and OER, due to their metallic conductivity and high surface area. Lead- and iridium-substituted $Pb_2Pb_xRu_{1-x}O_{6.5}$ and $Pb_2Ru_xIr_{1-x}O_{6.5}$ pyrochlores exhibited better catalytic activity for the ORR and OER and significantly higher stability during the OER than their unsubstituted counterparts.[30] The spinel oxides, especially cobaltites such as MCo_2O_4 (M = Co(II) and Ni(II)) and $CuCo_{3-x}O_4$, were also discovered to have activity for the ORR and OER in basic solutions, which was strongly dependent on the preparation procedure and the nature of the initial precursors.[31] Undoped and Li^+-doped $Co_{3-x}O_4$ spinel films prepared by a sol–gel low-temperature route had large surface areas and remarkable OER performance in 1 M KOH.[32] In general, ion-site substitution, which has been widely studied, and the size or surface nanocrystallization, which has been applied in some noble-metal bifunctional catalysts such as Pt and Ag,[33] can be considered as promising solutions to obtain applicable ORR and OER bifunctional catalysts.

♦ Comparison with Nonaqueous Lithium/Air Battery

Nonaqueous lithium/air rechargeable batteries have more simple construction and have higher energy than the aqueous lithium/air rechargeable batteries. However, nonaqueous lithium/air batteries have some disadvantages compared to aqueous lithium/air batteries. The oxygen electrode reaction is complex and still uncertain, because reactions (1) and (2) are accompanied by side reactions from decomposition of the electrolyte.[34] The product of the discharge reaction, Li_2O_2, is insoluble in aprotic solutions and, therefore, deposits on pore orifices on the surface of the air electrode, which decreases the usable pore volume for O_2 intake and stops the discharge process. In addition, high polarization is observed during charging.

These phenomena limit the energy density of the nonaqueous lithium/air battery. Moisture or CO_2 in the air will penetrate into the cell to contaminate aprotic electrolytes and react with the lithium metal and lithium salt, which degrades the cycling performance.[35]

Recently many researchers have attempted to improve the performance of the nonaqueous system. Gasteiger and coworkers found that Au/C had very high ORR activity, while Pt/C exhibited extraordinarily high OER activity in a 1 M $LiClO_4$ propylene carbonate (PC):dimethyl carbonate (DMC) electrolyte.[36] A mixture of PtAu nanoparticles exhibited bifunctional catalytic activity, increasing the discharge voltage to above 2.7 V and lowering the charge voltage below 3.5 V at 50 mA g^{-1}_{carbon}.[36] Ishihara et al. prepared a Pd–β-MnO_2 (mesoporous) catalyst using a SiO_2 template that also resulted in a significant reduction of the discharge and charge overpotential.[37] To improve the stability and cycling performance of the nonaqueous system, lithium-stable room-temperature ionic liquids (RTIL) are attractive materials. Some RTILs are nonvolatile and hydrophobic. Kuboki et al. reported an extremely high discharge capacity of 5360 mA h g^{-1} in a primary lithium/air battery using a hydrophobic RTIL of 1-ethyl-3-methylimidazolium bis(trifluoromethylsulfonyl)amide (EMITFSI) + 0.5 M LiTFSI at a current density of 0.01 mA cm^{-2}. The cell was operated for 56 days in air.[38] Recently, Iba et al. compared the electrochemical behavior of lithium/air batteries with PP13TFSI and PC electrolytes. The cell with the PP13TFSI electrolyte exhibited much lower polarization for the discharge and charge processes.[39] However; RTIL electrolytes also have some disadvantages, such as high viscosity, low ionic conductivity, lower stability of the lithium salt in air, and limited oxygen solubility.

♦ Conclusion

Lithium/air secondary batteries have received increased attention, motivated by urgency, due to environmental issues and the prospect of realizing EVs with high energy density batteries. Nonaqueous, aqueous, and even all-solid systems are under development. Each system has its own advantages and disadvantages, so that the future status has not been clearly defined until now. Here, the prospects and challenges in the development of aqueous lithium/air secondary batteries are summarized:

1) WSLEs are prerequisite in the development of aqueous lithium/air secondary batteries. The Li/polymer electrolyte/LTAP configuration is especially promising, due to the ease of preparation, flexibility, and compatibility of the polymer buffer layer with Li metal and LTAP plate. Further decrease of the interfacial resistance between lithium and the polymer electrolyte suppresses dendrite formation and increases the power density.

2) The water-stable protective layer is the key material of the WSLE. At present, only the NASICON-type LTAP is available as a protective layer. The mechanical properties and ionic conductivity should be improved by further research. A new class of high ionic conductivity solid electrolyte, the garnet-type $Li_7La_3Zr_2O_{12}$, is a good candidate for the protective layer.

3) Aqueous lithium/air rechargeable batteries using WSLEs are limited by evaporation of water during long operation; therefore, the challenges for aqueous electrolytes lie in suppressing evaporation to maintain operation during long-term operation. A possible method to address this would be to design a simple system to supply water.

4) A single catalytic layer with bifunctional catalytic activity for the ORR and OER will be developed using perovskite, spinel, or pyrochlore type oxide materials. Ion-site substitution and nanocrystallization of the particle size and surface are promising methods to improve the catalytic activity of these bifunctional catalysts. It should also be noted that the lithium/air batteries have rigorous requirement with respect to the electrochemical stability of bifunctional air cathodes, due to the high working voltage, especially during the charge process.

References and Notes

1 K. M. Abraham, Z. Jiang, *J. Electrochem. Soc.* **1996**, *143*, 1.
2 T. Ogasawara, A. Débart, M. Holzapfel, P. Novák, P. G. Bruce, *J. Am. Chem. Soc.* **2006**, *128*, 1390.
3 a) G. Girishkumar, B. McCloskey, A. C. Luntz, S. Swanson, W. Wilcke, *J. Phys. Chem. Lett.* **2010**, *1*, 2193. b) A. Kraytsberg, Y. Ein-Eli, *J. Power Sources* **2011**, *196*, 886.
4 S. J. Visco, E. Nimon, B. Katz, L. C. D. Jonghe, M. Y. Chu, The 12th International Meeting on Lithium Batteries Abstracts, Nara, Japan, **2004**, Abstr., No. 53.
5 J. Fu, U. S. Patent 5702995, **1997**; J. Fu, *J. Mater. Sci.* **1998**, *33*, 1549.
6 T. Zhang, N. Imanishi, A. Hirano, Y. Takeda, O. Yamamoto, *Electrochem. Solid-State Lett.* **2011**, *14*, A45.
7 S. J. Visco, Y. S. Nimon, B. D. Katz, U. S. Patent 7282296B2, **2007**.
8 U. von Alpen, M. F. Bell, T. Gladden, *Electrochim. Acta* **1979**, *24*, 741.
9 a) N. Imanishi, S. Hasegawa, T. Zhang, A. Hirano, Y. Takeda, O. Yamamoto, *J. Power Sources* **2008**, *185*, 1392. b) T. Zhang, N. Imanishi, S. Hasegawa, A. Hirano, J. Xie, Y. Takeda, O. Yamamoto, N. Sammes, *J. Electrochem. Soc.* **2008**, *155*, A965. c) T. Zhang, N. Imanishi, S. Hasegawa, A. Hirano, J. Xie, Y. Takeda, O. Yamamoto, N. Sammes, *Electrochem. Solid-State Lett.* **2009**, *12*, A132.
10 a) J. Fan, P. S. Fedkiw, *J. Electrochem. Soc.* **1997**, *144*, 399. b) G. B. Appetecchi, F. Croce, G. Dautzenberg, M. Mastragostino, F. Ronci, B. Scrosati, F. Soavi, A. Zanelli, F. Alessandrini, P. P. Prosini, *J. Electrochem. Soc.* **1998**, *145*, 4126. c) F. Croce, G. B. Appetecchi, L. Persi, B. Scrosati, *Nature* **1998**, *394*, 456.
11 S. Liu, N. Imanishi, T. Zhang, A. Hirano, Y. Takeda, O. Yamamoto, J. Yang, *J. Electrochem. Soc.* **2010**, *157*, A1092.
12 a) K. Brandt, *Solid State Ionics* **1994**, *69*, 173. b) R. Selim, P. Bro, *J. Electrochem. Soc.* **1974**, *121*, 1457. c) I. Yoshimatsu, T. Hirai, J. Yamaki, *J. Electrochem. Soc.* **1988**, *135*, 2422.
13 H. E. Park, C. H. Hong, W. Y. Yoon, *J. Power Sources* **2008**, *178*, 765.
14 a) C. Brissot, M. Rosso, J.-N. Chazalviel, P. Baudry, S. Lascaud, *Electrochim. Acta* **1998**, *43*, 1569. b) M. Rosso, C. Brissot, A. Teyssot, M. Dollé, L. Sannier, J.-M. Tarascon, R. Bouchet, S. Lascaud, *Electrochim. Acta* **2006**, *51*, 5334.
15 S. Liu, N. Imanishi, T. Zhang, A. Hirano, Y. Takeda, O. Yamamoto, J. Yang, *J. Power Sources* **2010**, *195*, 6847.
16 a) S. Hasegawa, N. Imanishi, T. Zhang, J. Xie, A. Hirano, Y. Takeda, O. Yamamoto, *J. Power Sources* **2009**, *189*, 371. b) Y. Shimonishi, T. Zhang, P. Johnson, N. Imanishi, A. Hirano, Y. Takeda, O. Yamamoto, N. Sammes, *J. Power Sources* **2010**, *195*, 6187. c) Y. Shimonishi, T. Zhang, A. Hirano, N. Imanishi, Y. Takeda, O. Yamamoto, N. Sammes, *Solid State Ionics*, in press.
17 T. Zhang, N. Imanishi, Y. Shimonishi, A. Hirano, Y. Takeda, O. Yamamoto, N. Sammes, *Chem. Commun.* **2010**, *46*, 1661.
18 R. Murugan, V. Thangadurai, W. Weppner, *Angew. Chem., Int. Ed.* **2007**, *46*, 7778.
19 Y. Shimonishi, A. Toda, T. Zhang, A. Hirano, N. Imanishi, O. Yamamoto, Y. Takeda, *Solid State Ionics* **2011**, *183*, 48.
20 M. Kotobuki, H. Munakata, K. Kanamura, Y. Sato, T. Yoshida, *J. Electrochem. Soc.* **2010**, *157*, A1076.
21 Q. Li, N. Imanishi, A. Hirano, Y. Takeda, O. Yamamoto, *J. Power Sources* **2002**, *110*, 38.
22 H. Zhou, Y. Wang, H. Li, P. He, *ChemSusChem* **2010**, *3*, 1009.
23 Y. Wang, H. Zhou, *Chem. Commun.* **2010**, *46*, 6305.
24 H. Li, Y. Wang, H. Na, H. Liu, H. Zhou, *J. Am. Chem. Soc.* **2009**, *131*, 15098.
25 L. Carlsson, L. Öjefors, *J. Electrochem. Soc.* **1980**, *127*, 525.
26 T. Burchardt, U. S. Patent 20070166602, **2007**.
27 Y. Shimizu, H. Matsuda, N. Miura, N. Yamazoe, *Chem. Lett.* **1992**, 1033.
28 T. Hyodo, Y. Shimizu, N. Miura, N. Yamazoe, *Denki Kagaku* **1994**, *62*, 158.
29 Y. Shimizu, A. Nemoto, T. Kyodo, N. Miura, N. Yamazoe, *Denki Kagaku* **1993**, *61*, 1458.
30 L. Jörissen, *J. Power Sources* **2006**, *155*, 23.
31 J. Prakash, D. A. Tryk, W. Aldred, E. B. Yeager, *J. Appl. Electrochem.* **1999**, *29*, 1463.
32 a) F. Švegl, B. Orel, I. Grabec-Švegl, V. Kaučič, *Electrochim. Acta* **2000**, *45*, 4359. b) V. Nikolova, P. Iliev, K. Petrov, T. Vltanov, E. Zhecheva, R. Stoyanova, I. Valov, D. Stoychev, *J. Power Sources* **2008**, *185*, 727.
33 T. Wang, M. Kaempgen, P. Nopphawan, G. Wee, S. Mhaisalkar, M. Srinivasan, *J. Power Sources* **2010**, *195*, 4350.
34 a) A. Débart, A. J. Paterson, J. Bao, P. G. Bruce, *Angew. Chem., Int. Ed.* **2008**, *47*, 4521. b) F. Mizuno, S. Nakanishi, Y. Kotani, S. Yokoishi, H. Iba, *Electrochemistry* **2010**, *78*, 403.
35 S. R. Younesi, K. Ciosek, K. Edstrom, The Electrochemical Society Meeting Abstracts, Honolulu, HI, **2008**, Vol. 214, Abstr., No. 0465.
36 a) Y.-C. Lu, H. A. Gasteiger, M. C. Parent, V. Chiloyan, Y. Shao-Horn, *Electrochem. Solid-State Lett.* **2010**, *13*, A69. b) Y.-C. Lu, Z. Xu, H. A. Gasteiger, S. Chen, K. Hamad-Schifferli, Y. Shao-Horn, *J. Am. Chem. Soc.* **2010**, *132*, 12170.
37 T. Ishihara, A. K. Thapa, Y. Hidaka, S. Ida, The 51th Battery Symposium in Japan Abstracts, Nagoya, Japan, **2010**, Abstr., No. 3B02.
38 T. Kuboki, T. Okuyama, T. Ohsaki, N. Takami, *J. Power Sources* **2005**, *146*, 766.
39 F. Mizuno, H. Iba, The 51th Battery Symposium in Japan Abstracts, Nagoya, Japan, **2010**, Abstr., No. 3B06.
40 Supporting Information is available electronically on the CSJ-Journal Web site, http://www.csj.jp/journals/chem-lett/index.html.

